965 **Supplementary Materials:**

966 Figures S1-S18

967 Table S1

Supplementary Materials for

Substrate processing by the Cdc48 ATPase complex is initiated by ubiquitin unfolding

Edward C. Twomey[1]*, Zhejian Ji[1]*, Thomas E. Wales[2], Nicholas O. Bodnar[1], Scott B. Ficarro[3,4], Jarrod A. Marto[3,4], John R. Engen[2], and Tom A. Rapoport[1#]

correspondence to: tom_rapoport@hms.harvard.edu

This PDF file includes:

Figs. S1 to S18
Table S1

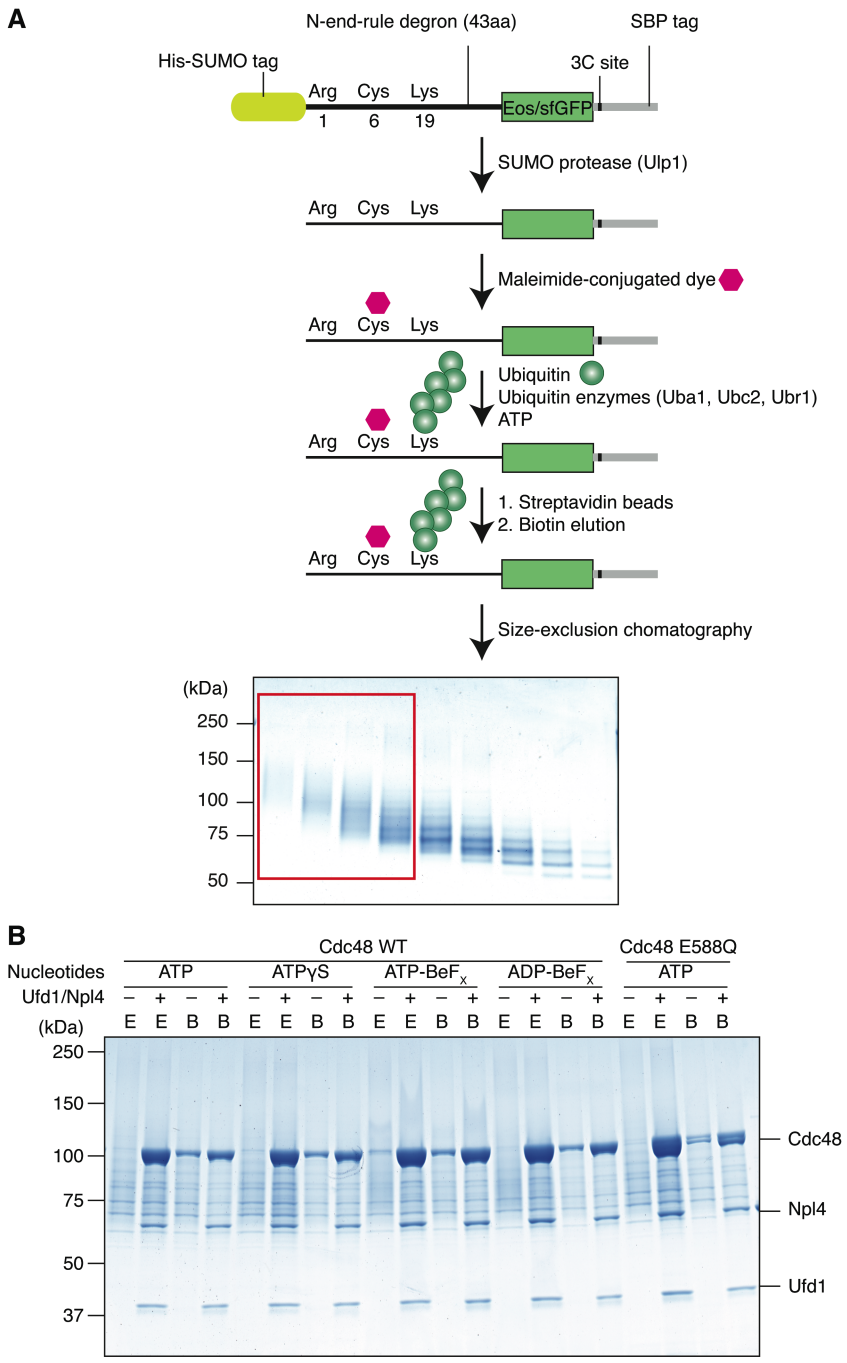

Fig. S1. Generation of poly-ubiquitinated substrate and of substrate-engaged Cdc48 ATPase complex.

(**A**) Scheme for the generation of poly-ubiquitinated substrate. The substrate consists of a His14-SUMO tag, a 43 amino acid degron sequence derived from the *E. coli* lac repressor, the fluorescent protein Eos or sfGFP, a 3C-cleavage site, and a streptavidin binding peptide (SBP) tag. The protein was purified on the basis of the N-terminal His14-tag, and the SUMO tag was then cleaved off with SUMO protease (Ulp1). In some experiments, a fluorescent dye was attached to Cys6. The protein was incubated with a

mixture of ubiquitin-activating enzyme (Uba1), ubiquitin-conjugating enzyme (Ubc2), ubiquitin ligase (Ubr1), ubiquitin, and ATP. The poly-ubiquitinated substrate was purified on streptavidin beads via its C-terminal SBP tag, eluted from the resin with biotin, and subjected to size-exclusion chromatography. Fractions were analyzed by SDS-PAGE and Coomassie blue staining. The fractions indicated with a red box were pooled and used to generate the substrate-engaged Cdc48 complex. (**B**) Substrate generated as in (**A**) was bound to streptavidin beads, incubated with or without Ufd1/Npl4 complex, and then with Cdc48 in the presence of the indicated nucleotides. Biotin was added and the eluted (E) and bound (B) fractions were analyzed by SDS-PAGE and Coomassie blue staining.

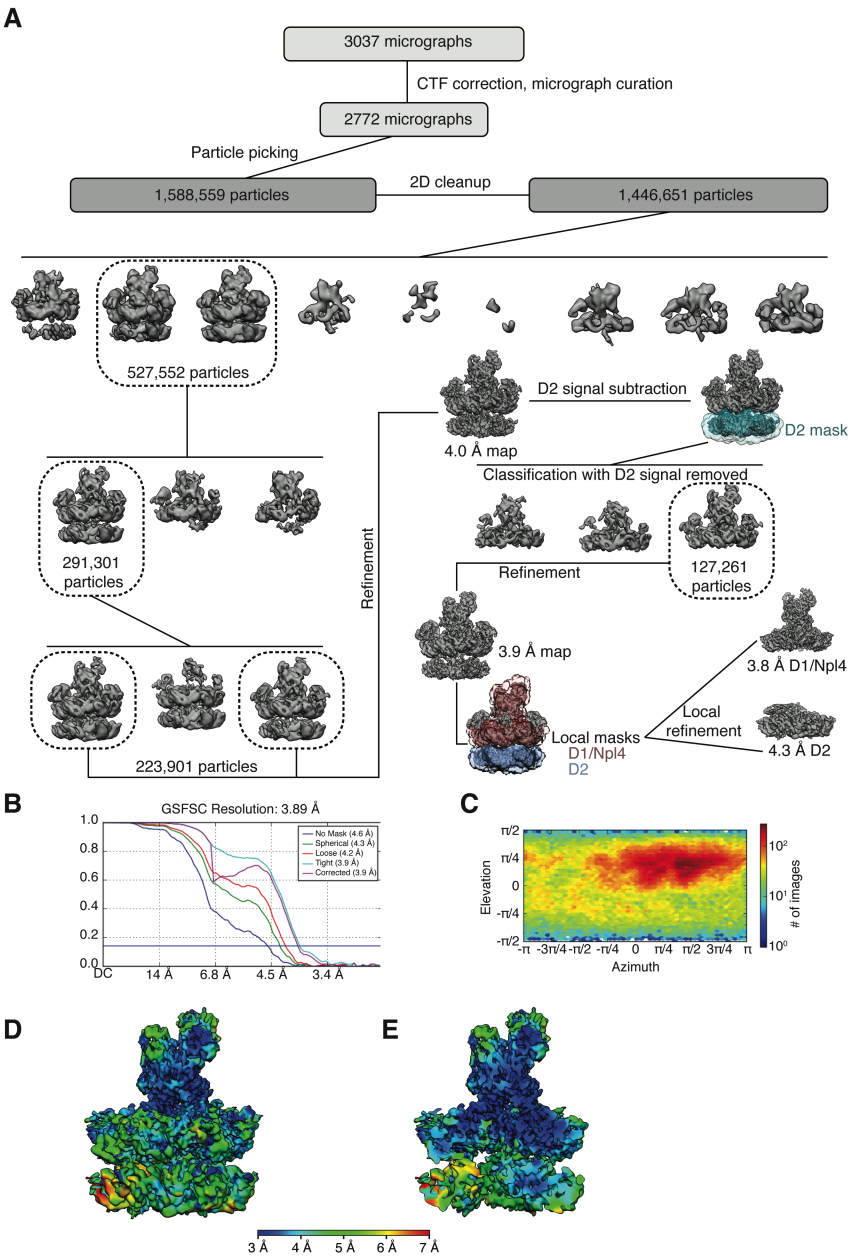

Fig. S2. Cryo-EM analysis of the substrate-engaged Cdc48 complex in ATP.

(**A**) Image processing workflow for 3D classification and refinement. Shown are side views of 3D reconstructions, with the number of particles used for further analysis indicated. (**B**) Gold-standard Fourier shell correlation (GSFSC) was calculated during refinement with different masks in Cryosparc2. The resolutions were determined at FSC=0.143. The final corrected mask gave an overall resolution of 3.9Å. (**C**) Direction distribution over azimuth and elevation angles of particles used in CryoSPARC refinement; (0,0) is a side view. (**D**) Side view of the map, with local resolution calculated from the unfiltered half-maps, colored according to the scale. (**E**) As in (**D**), but the density was cut to the central ATPase pore.

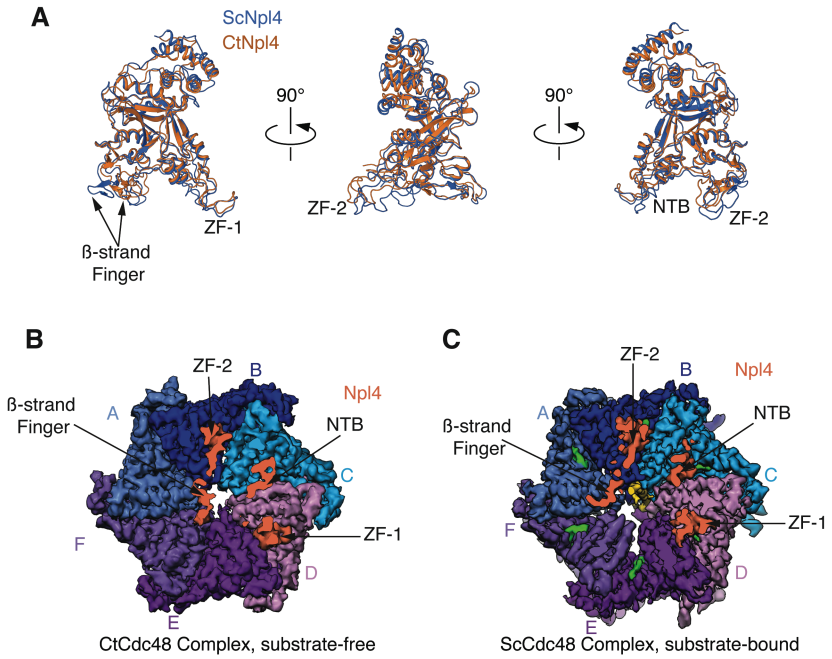

57
58

59 **Fig. S3. Comparison of the *S. cerevisiae* and *C. thermophilum* Npl4 towers and their**
60 **interaction with Cdc48.**

61 (**A**) Three different side views of the superimposed models of the Npl4 towers of the
62 substrate-engaged *S. cerevisiae* (Sc; blue) Cdc48 complex and substrate-free *C.*
63 *thermophilum* Cdc48 complex (Ct; orange; PDB code 6CDD). The models are shown in
64 ribbon representation. The b-strand finger, Zn^{2+}-fingers 1 and 2 (ZF-1 and ZF-2), and N-
65 terminal bundle (NTB) are indicated. (**B**) Top view of the density map of the *C.*
66 *thermophilum* Cdc48 complex lacking substrate, cut close to the surface of the D1 ring.
67 Density for the Npl4 tower is shown in orange. (**C**) As in **(B)**, but for the substrate-
68 engaged *S. cerevisiae* complex. Note that the b-strand finger has moved outwards from
69 the pore.
70
71

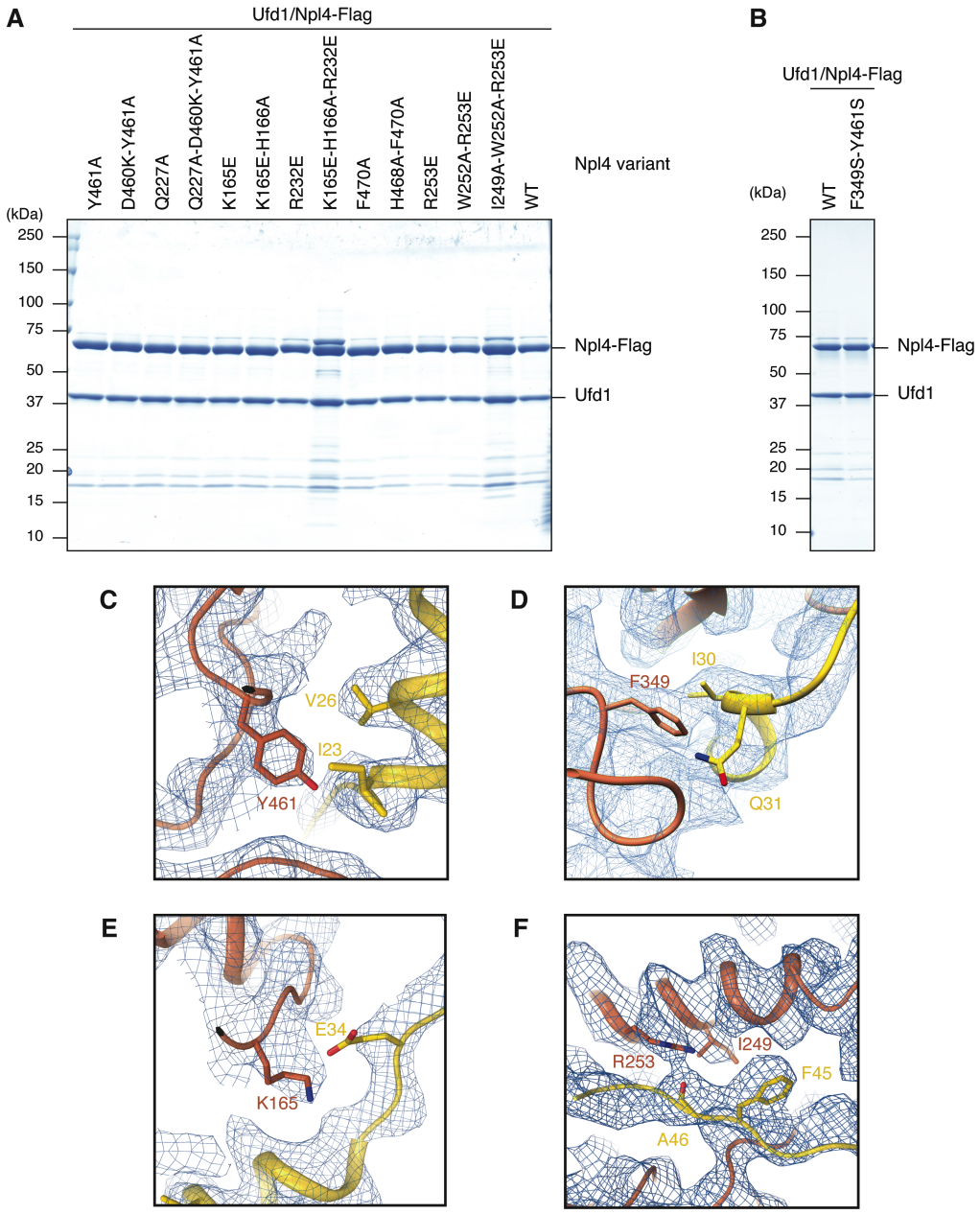

Fig. S4. Interaction of Npl4 mutants with Ufd1 and of Npl4 groove residues with unUb.

(**A-B**) Mutation of the Npl4 groove does not affect the interaction between Npl4 and Ufd1. Wild-type Npl4 or the indicated Npl4 mutants, all carrying FLAG-tags at the C-terminus, were co-expressed with His-SUMO Ufd1 in *E. coli*. The proteins were purified on the basis of the His-tag on Ufd1 and the tag was removed with SUMO-protease. The samples were analyzed by SDS-PAGE and Coomassie blue staining. (**C**) The conserved Y461 residue of Npl4 (orange) interacts with V26 and I23 of unUb (yellow). The models are shown in ribbon representation and the density as a blue mesh. (**D**) As in (**C**), but showing the interaction of F349 with I30 and Q31. (**E**) As in (**C**), but showing interaction

between K165 and E34. (**F**) As in (**C**), but showing interaction of R253 with the backbone of A46 and of I249 with F45.

87
88

(Continued on next page)

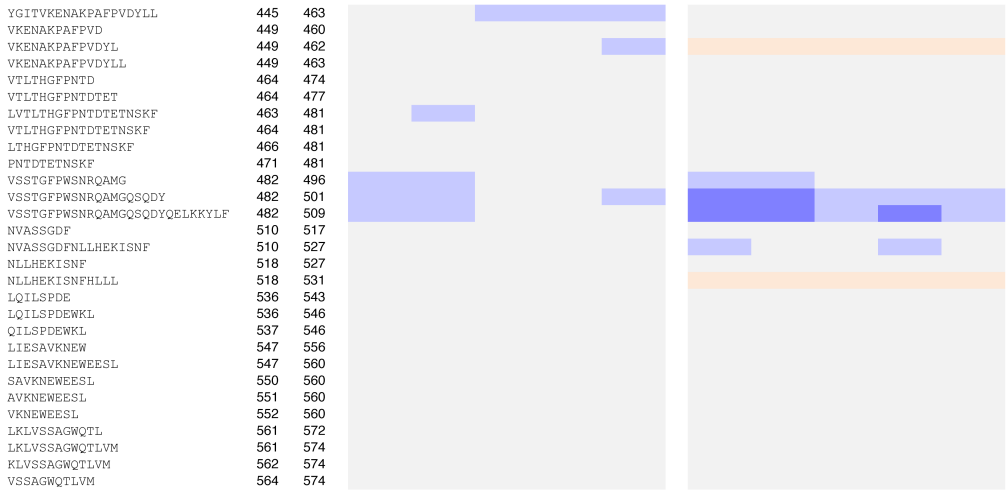

Fig. S5. Substrate protection of Npl4 from HDX in the absence or presence of Cdc48.

HDX was performed with Cdc48/UN complex and ADP/BeF_x (left) or with UN alone (right), in the absence or presence of substrate. The HDX reaction was quenched at different time points, the protein was digested with pepsin and the peptides analyzed by MS. Shown is the difference in HDX (with/without substrate) for peptides of Npl4. Shown is the mean of two experiments. The peptides are listed from the N- to the C-terminus, with their first and last residue indicated. The degree of HDX protection by substrate is shown in shades of blue (protection) and green (de-protection) (in Daltons, scale on the right).


Cdc48/UN/Substrate with ADP-BeFx -
Cdc48/UN with ADP-BeFx
Time (min)
Sequence
Start
End
0.167
1
10
60
311
UT3
UT6
SSFGGGNG 6 13
SSFGGGNGF 6 14
FVNMPQTF 14 21
VNMPQTF 15 21
VNMPQTFEEF 15 24
FFRCYPIAM 24 32
FRCYPIAM 25 32
MNDRIRKDDANFGGKIFLPPSAL 33 55
RIRKDDANFGGKIFLPPSAL 36 55
FGGKIFLPPSAL 44 55
GGKIFLPPSAL 45 55
LNIRYPML 61 68
NIRYPML 62 68
FKLTANETGRVTHGGVL 69 85
FKLTANETGRVTHGGVLE 69 86
FKLTANETGRVTHGGVLEF 69 87
KLTANETGRVTHGGVLE 70 86
TANETGRVTHGGVLEF 72 87
IAEEGRVYLPQWM 88 100
IAEEGRVYLPQWMM 88 101
EGRVYLPQW 91 99
EGRVYLPQWM 91 100
GRVYLPQWM 92 100
GRVYLPQWMM 92 101
RVYLPQWM 93 100
RVYLPQWMM 93 101
METLGIQPGSL 101 111
GIQPGSL 105 111
LQISSTDVPLGQ 112 123
LQISSTDVPLGQF 112 124
DVPLGQF 118 124
FVKLEPQSVDF 124 134
FVKLEPQSVDFL 124 135
VKLEPQSVDF 125 134
VKLEPQSVDFL 125 135
LDISDPKAVL 135 144
LDISDPKAVLENVLRNFSTL 135 154
ENVLRNFSTL 145 154
VLRNFSTL 147 154
TVDDVIE 155 161
ISYNGKTF 162 169
ISYNGKTFKIKIL 162 174
SYNGKTFKIKILEVKPESSSKSIC 163 186
FKIKILEVKPESSSKSIC 169 186
FKIKILEVKPESSSKSICV 169 187
VTDFAPPVG 193 201
LVTDFAPPVGYVEPDY 192 207
VTDFAPPVGYVEPDY 193 207
DFAPPVGYVEPDY 195 207
LVTDFAPPVGYVEPDYKALKAQQDKEKKNSFGKGQVLDPSVL 192 233
VTDFAPPVGYVEPDYKALKAQQDKEKKNSFGKGQVLDPSVL 193 233
KALKAQQDKEKKNSFGKGQVLDPSVL 208 233
KALKAQQDKEKKNSFGKGQVLDPSVLGQGSM 208 238
GQGSMST 234 240
STRIDYAGIANSSRNKLSKF 239 258
RIDYAGIANSSRNKLSKF 241 258
VGQGQNISGKAPKAEPKQDIKD 259 280
GQGQNISGKAPKAEPKQDIKD 260 280
ISGKAPKAEPKQDIKD 265 280
DGEPAKL 286 292
MKITFDGEPAKLDLPEGQL 281 299
MKITFDGEPAKLDLPEGQLF 281 300
EPAKLDLP 288 295
DGEPAKLDLPEGQL 286 299
DGEPAKLDLPEGQLF 286 300
DLPEGQL 293 299
FGFPMVL 301 307
PMVLPKEDEES 304 314
PMVLPKEDEESAAGSKSSEQNF 304 325
PMVLPKEDEESAAGSKSSEQNFQGQG 304 329
PKEDEESAAGSKSSEQNF 308 325
PKEDEESAAGSKSSEQNFQGQG 308 329
PKEDEESAAGSKSSEQNFQGQGISL 308 332
DEESAAGSKSSEQNFQGQGISL 311 332
QGQGISL 326 332
RKSNKRKTKSDHDSS 333 347
RKSNKRKTKSDHDSSKSKAPKSPEV 333 357
PKSPEVIE 352 359
APKSPEVIEID 351 361
5.0
2.5
0
- 2.5
- 5.0
No data

Fig. S6. Substrate protection from HDX determined for Ufd1 in the Cdc48/UN complex.

HDX was performed with a Cdc48/UN complex and ADP/BeF_x in the absence or presence of substrate. The HDX reaction was quenched at different time points, the protein was digested with pepsin and the peptides analyzed by MS. Shown is the difference in HDX (with/without substrate) for peptides of Ufd1. Shown is the mean of two experiments. The peptides are listed from the N- to the C-terminus, with their first and last residue indicated. The degree of HDX protection by substrate is shown in shades of blue (protection) and green (de-protection) (in Daltons, scale on the right). Peptides belonging to the UT3 and UT6 domains of Ufd1 are indicated by the bars on the left.

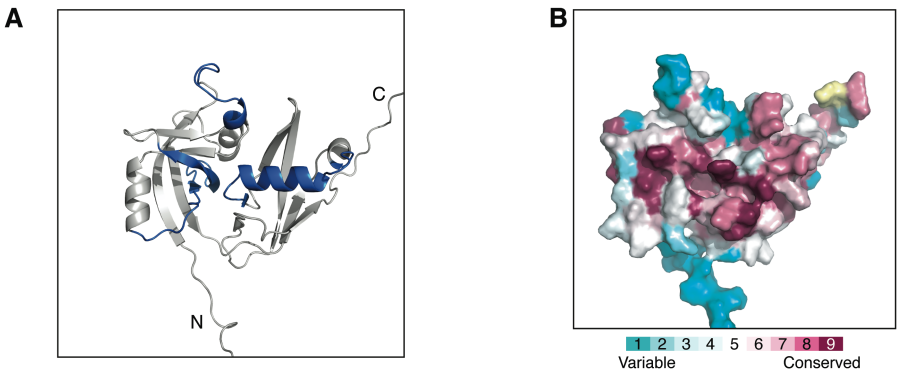

Fig. S7. Substrate binding to the UT3 domain of Ufd1 analyzed by HDX MS.

(**A**) HDX MS was performed with Cdc48/UN/ADP/BeF_x in the absence or presence of poly-ubiquitinated substrate at different time points (**fig. S6**). Substrate-protected regions in the UT3 domain are shown in blue in a ribbon representation of its NMR structure (PDB code: 1ZC1). (**B**) Surface model of UT3 viewed as in (**A**). Residues are colored according to the degree of their conservation. Regions in yellow had insufficient sequences for calculation of their conservation (less than 10%). The conservation map was generated by the ConSurf Server.

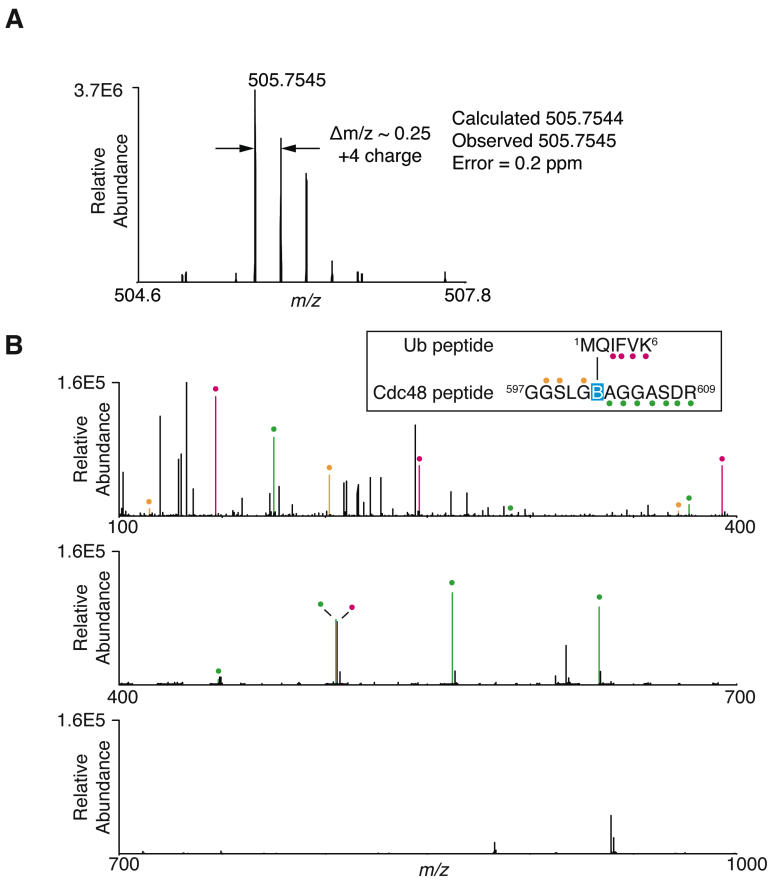

Fig. S8. Identification of photo-crosslinks between Cdc48 and ubiquitin by mass spectrometry.

(A) Cdc48-FLAG containing benzoylphenylalanine (Bpa) at position 602 was incubated with UN and dye-labeled, poly-ubiquitinated sfGFP in the presence of ADP. The sample was irradiated, and Cdc48-FLAG and crosslinked products were isolated with FLAG-antibody beads. Nano LC-MS/MS analysis of tryptic digests resulted in detection of a quadruply charged precursor ion at *m/z* 505.7545 consistent with the mass of ^{597}GGSLG(Bpa)AGGASDR^{609} (Cdc48) crosslinked to ^{1}MQIFVK^{6} (ubiquitin). **(B)** MS/MS spectrum of the crosslinked peptide precursor described in (**A**). Cdc48 derived ions of type b and y are marked with yellow and green glyphs, respectively, while y-type ions derived from ubiquitin are marked with magenta glyphs. B, Bpa.

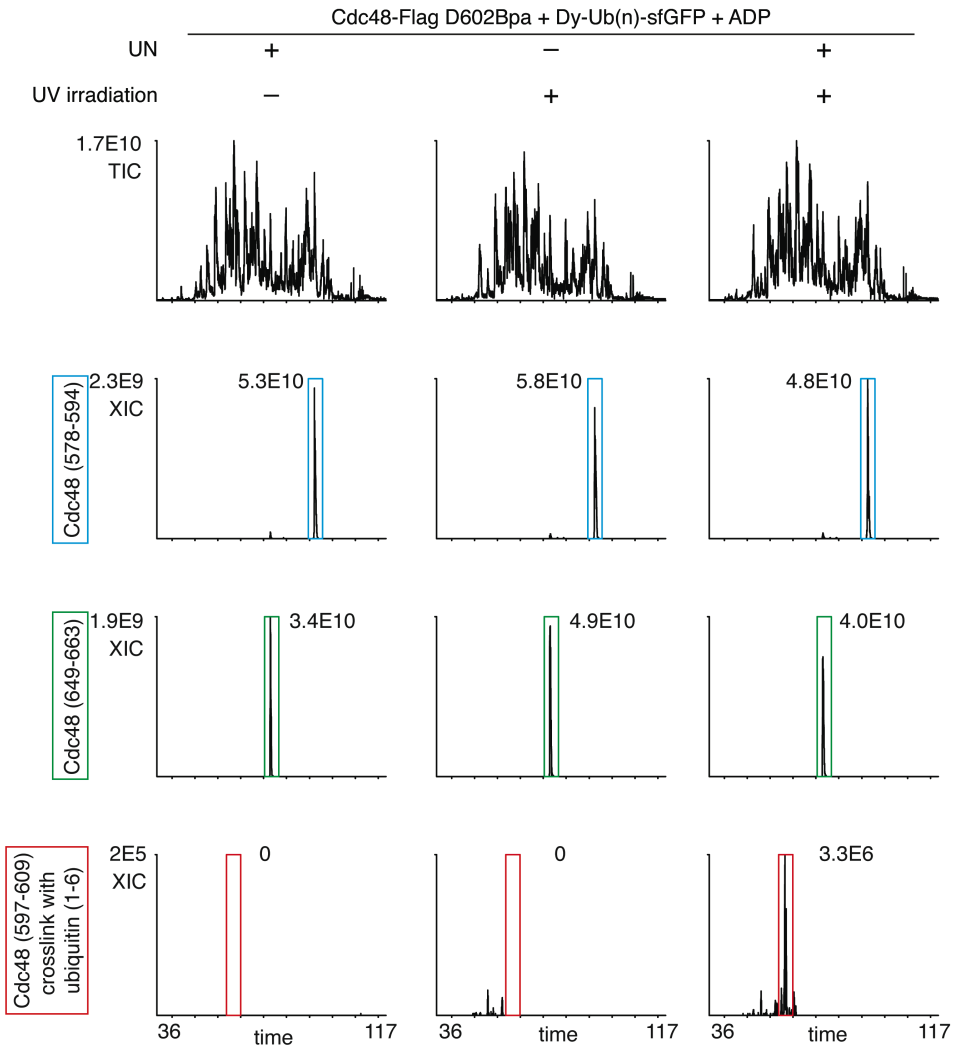

144
145

146 **Fig. S9. Crosslinking between Cdc48 and ubiquitin is dependent on the presence of**
147 **UN and irradiation.**

148 Total ion chromatograms (TICs) and extracted ion chromatograms (XICs) obtained
149 during nano-LC-MS/MS of tryptic digests of crosslinking reactions. Crosslinking was
150 performed as described in **fig. S8**. Reaction 1 (left column) was not irradiated, reaction 2
151 (middle column) was performed without UN, and reaction 3 (right column) was
152 irradiated in the presence of UN. Reference peptides from Cdc48 (residues 578-594, blue
153 rectangle; residues 649-663, green rectangle) were detected at similar levels in each
154 reaction, while the peptide ^{597}GGSLG(Bpa)AGGASDR^{609} (Cdc48) crosslinked to
155 ^{1}MQIFVK^{6} (ubiquitin) was detected only after UV irradiation and in the presence of UN
156 (reaction 3, right column, red rectangle). The peak area for each peptide is indicated
157 within each XIC.
158
159

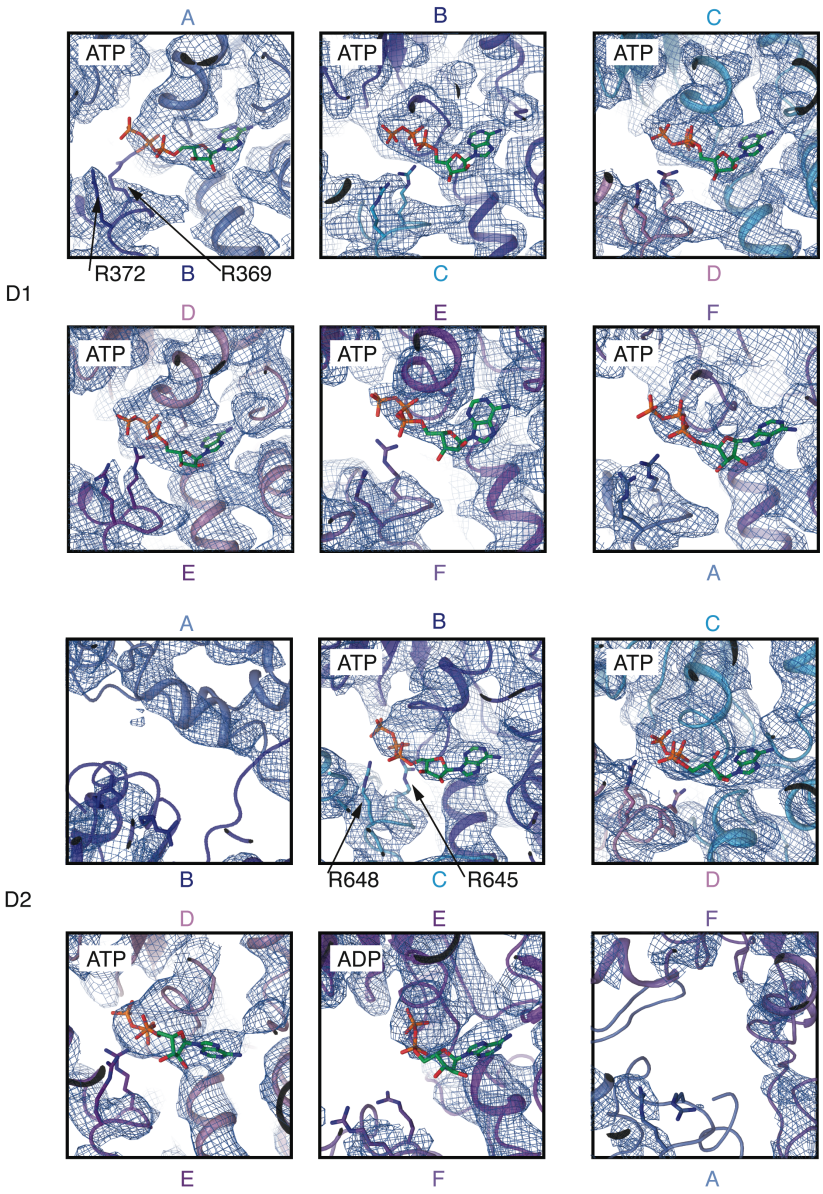

Fig. S10. Nucleotides bound to the substrate-engaged Cdc48 complex prepared in ATP.

Nucleotide binding pockets of the ATPase subunits in the D1 and D2 rings. Density for the nucleotide and neighboring protein segments are shown as a blue mesh. Models for protein are shown in ribbon representation and the nucleotides as stick models. Arg residues contacting the nucleotide from the neighboring ATPase subunits are indicated. The assignment of ADP or ATP is based on comparing nucleotide densities and the presence or absence of an Arg finger of the neighboring subunit in its vicinity. In the D2 ring, the nucleotide binding pockets of subunits A and F are wide open. These subunits are probably in the nucleotide-free state.

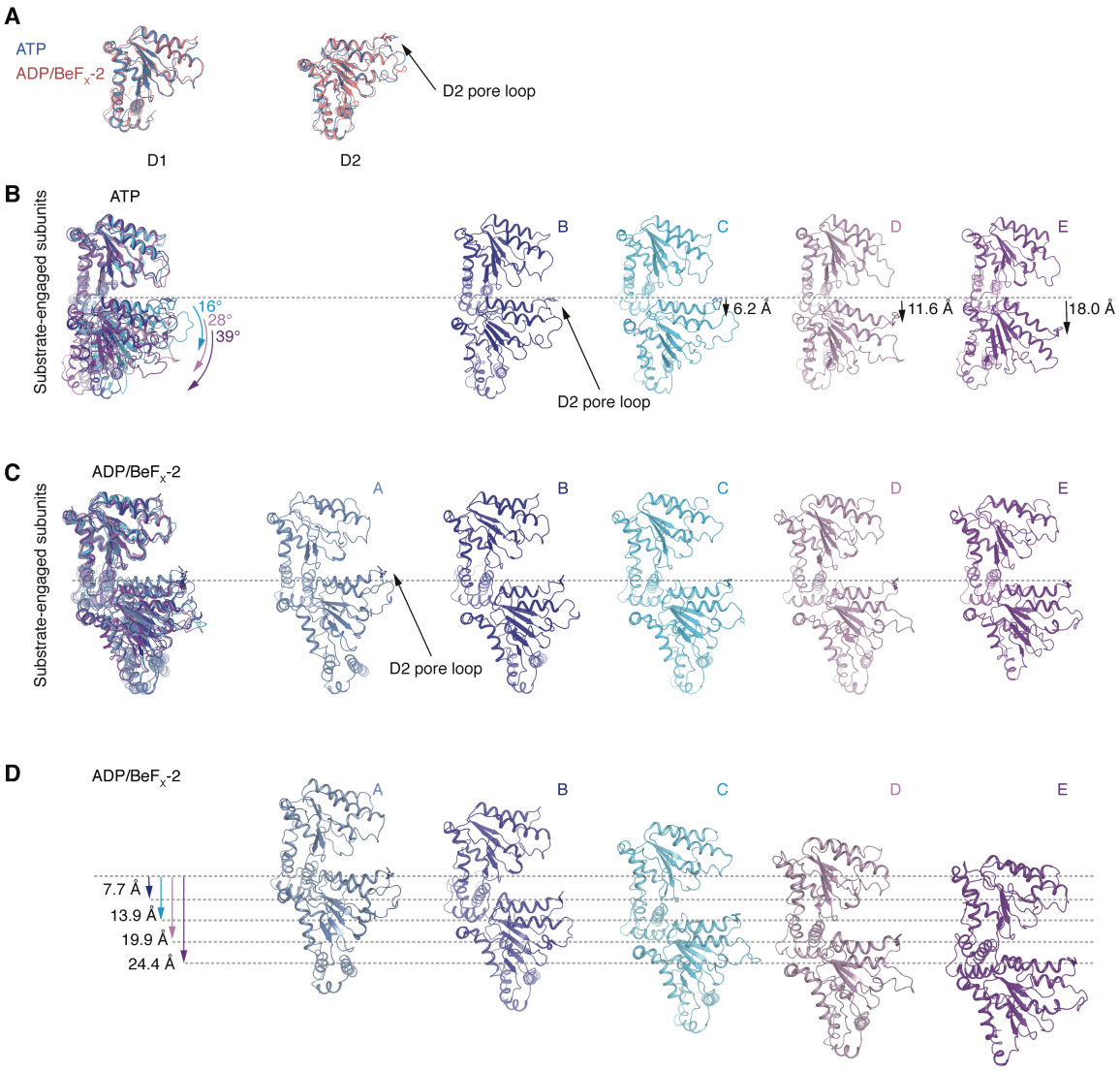

Fig. S11. The D1 and D2 domains of the Cdc48 monomers behave as rigid bodies. **(A)** Superposition of D1 and D2 domains from ATP and ADP/ BeF_x -2 structures. **(B)** The substrate-engaged Cdc48 monomers from the ATP structure were superimposed using the D1 domains as reference. The D2 domains of monomers B-E move as rigid bodies. The angles and distances of the D2 pore loop changes are indicated. **(C)** As in **(B)**, but for the ADP/BeFx-2 structure. Note that the relative positions of the D1 and D2 domains remains unchanged among the monomers. **(D)** Changes of the substrate engaged monomers A-E in the ADP/BeF_x-2 structure. D1 and D2 move together the indicated distances.

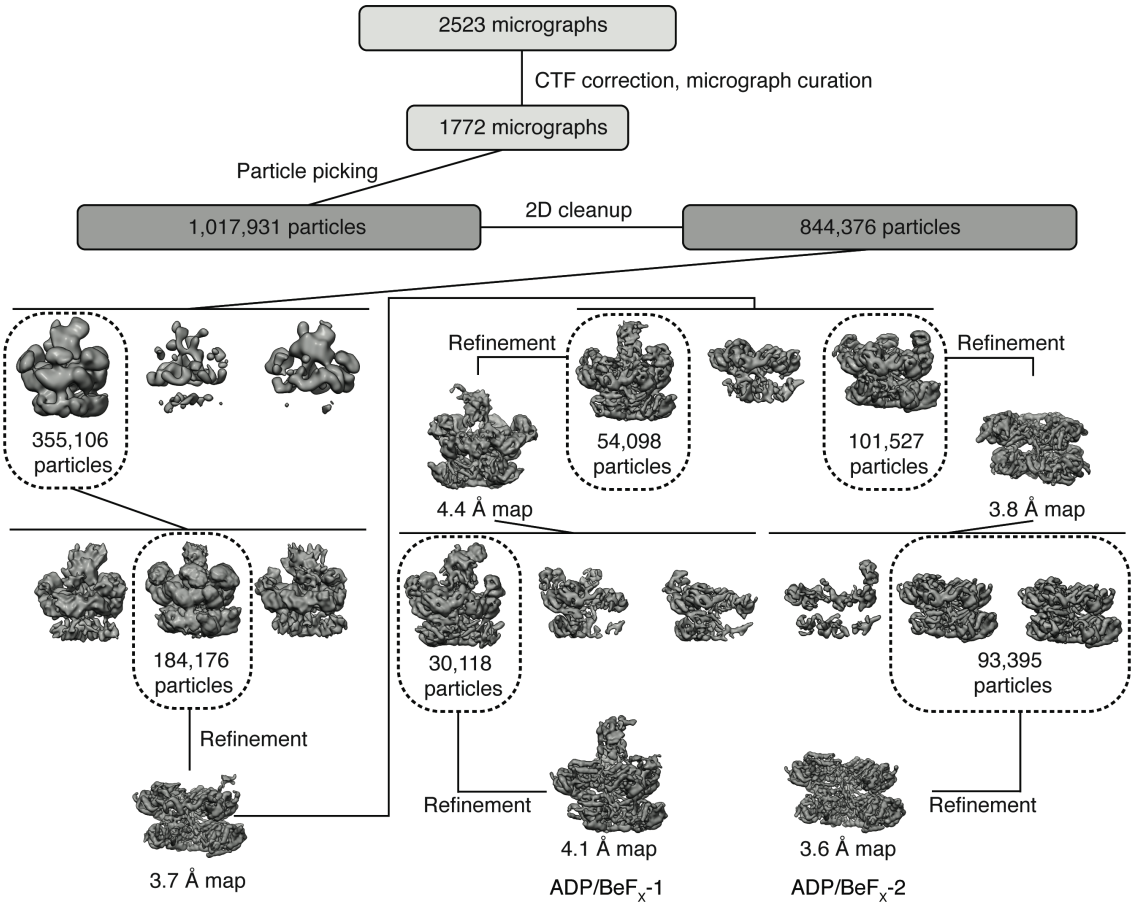

Fig. S12. Cryo-EM analysis of the substrate-engaged Cdc48 complex in ADP/BeF_x.
Image processing workflow for 3D classification and refinement. Shown are side views of 3D reconstructions, with the number of the particles used for further analysis indicated. The two best classes (ADP/BeF_x-1 and ADP/BeF_x-2) had final overall resolutions of 4.1Å and 3.7Å, respectively.

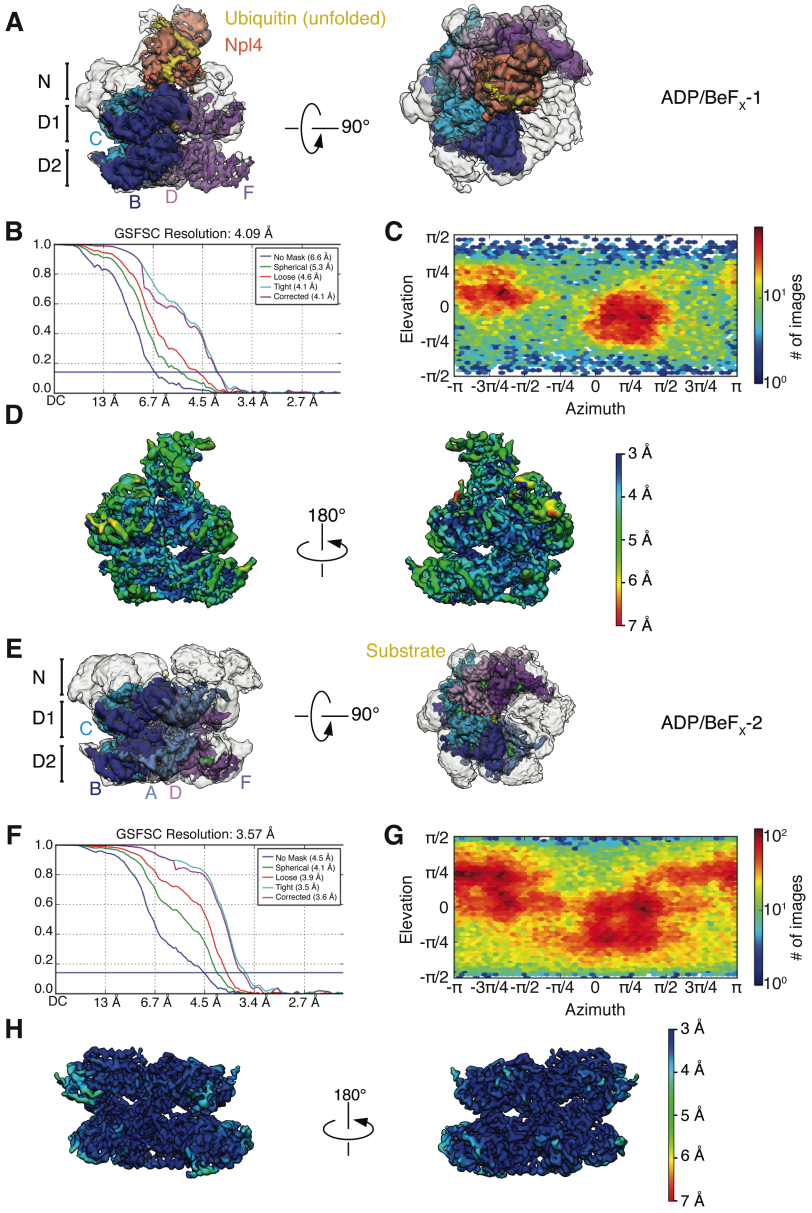

196
197

198 **Fig. S13. Refined cryo-EM maps of the substrate-engaged Cdc48 complex in**
199 **ADP/BeF$_x$.**

200 (**A**) Cryo-EM map of the 3D class ADP/BeFx-1 in two different views. The domains of
201 Cdc48, cofactor, and ubiquitin molecules attached to substrate are shown in different
202 colors. The subunits in the hexameric ATPase ring are labeled. The refined, unsharpened
203 map is shown in transparent grey over the final map sharpened with a B-factor of -150.
204 (**B**) Gold-standard Fourier shell correlation (GSFSC) calculated during refinement with
205 different masks in Cryosparc2. The resolutions were determined at FSC=0.143. The final
206 corrected mask gave an overall resolution of 3.9Å. (**C**) Direction distribution over
207 azimuth and elevation angles of particles used in CryoSPARC refinement; (0,0) is a side
208 view. (**D**) Local resolution was calculated from the unfiltered half-map and colored

according to the scale on the side. (**E**)-(**H**) As in (**A**)-(**D**), but for the 3D class ADP/BeFx-2. The ADP/BeF_x-2 map was sharpened with a B-factor of -100. The final corrected mask gave an overall resolution of 3.6Å.

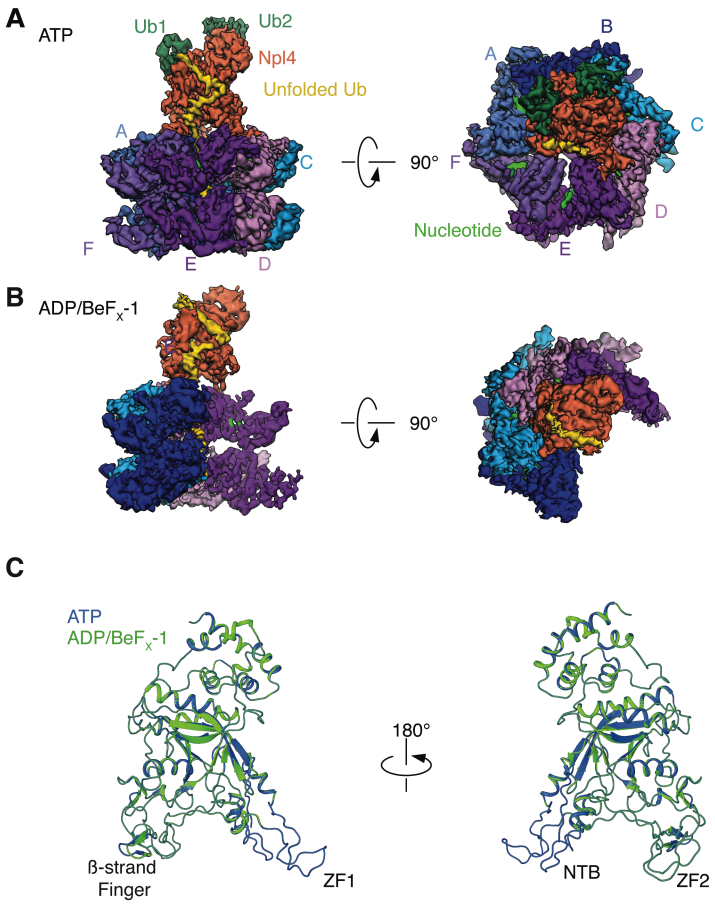

Fig. S14. Comparison of the Npl4 towers in the ATP and ADP/BeF_x-1 structures.
(**A**) Side and top views of a sharpened map (B-factor = -150) of the substrate-engaged Cdc48 complex in ATP. (**B**) As in (**A**), but for the ADP/BeF_x-1 map. (**C**) Ribbon diagram models for the Npl4 tower in the ATP (blue) and ADP/BeF_x-1 (green) structures. Note that no density for Zn^{2+}-finger 1 (ZF-1) and the N-terminal bundle (NTB) were seen in the ADP/BeF_x-1 map, likely because these domains are not associated with Cdc48.

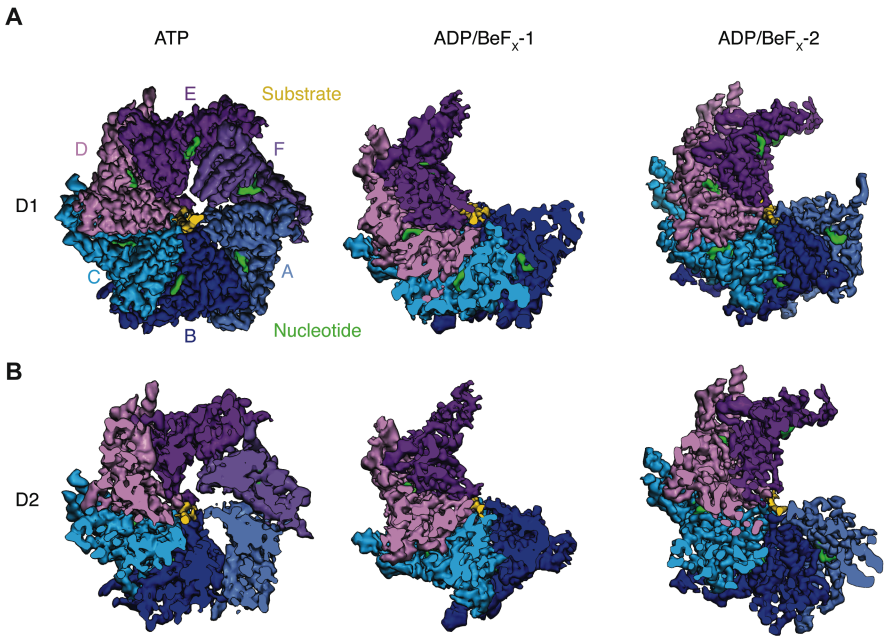

224
225

226 **Fig. S15. Comparison of the maps for the D1 and D2 ATPase rings in the three cryo-**
227 **EM reconstructions.**

228 **(A)** Top view of the density maps of the ATP, ADP/BeF$_x$ -1, and ADP/BeF$_x$ -2 structures,
229 cut to the surface of the D1 ring. Substrate density is shown in yellow. The D1 ATPases
230 are colored individually and labeled A-F. Density for bound nucleotides is shown in
231 green. (**B**) As in (**A**), but cut to the surface of the D2 ring. Note that the gaps in the D1
232 and D2 rings of the ADP/BeF$_x$-1, and ADP/BeF$_x$-2 structures, corresponding to flexible
233 ATPase subunits, are at the same positions.
234
235

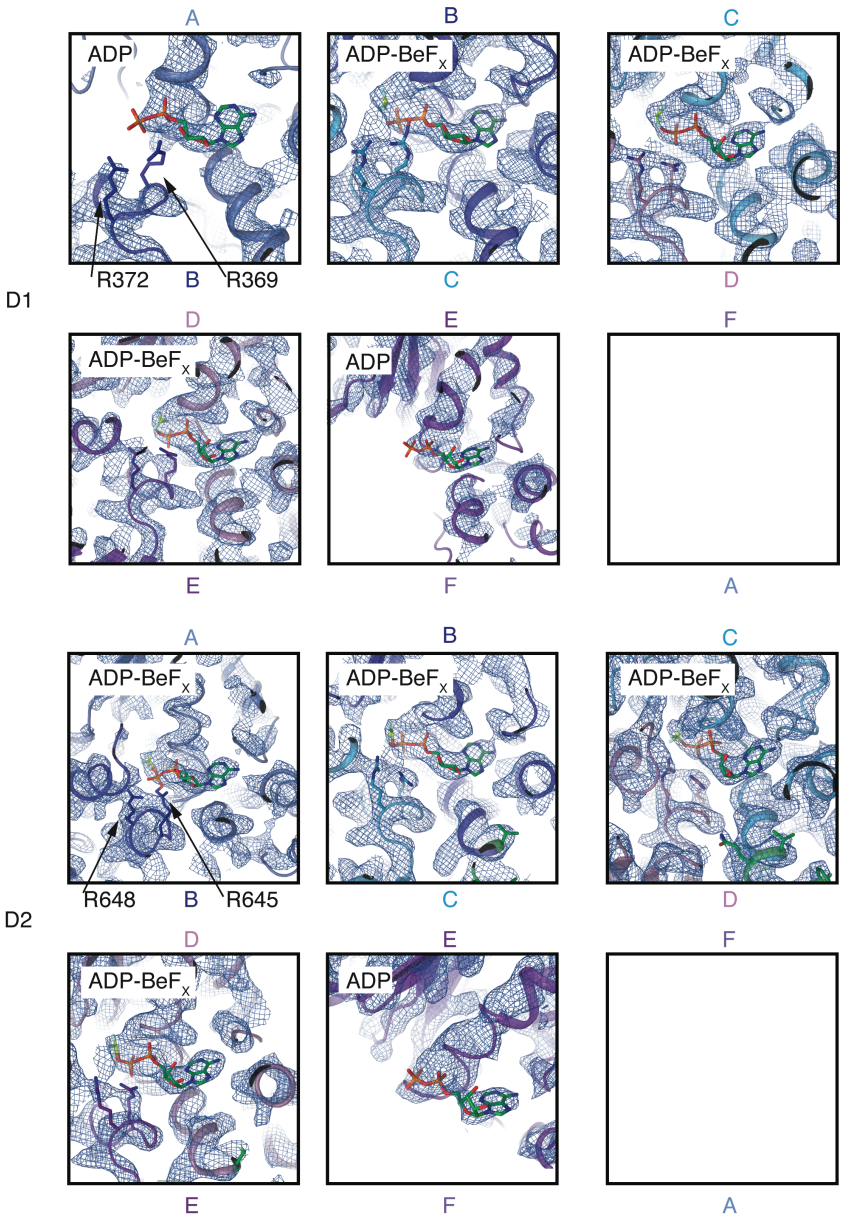

Fig. S16. Nucleotides bound in the ADP/BeF$_x$-2 structure.

Nucleotide binding pockets of the ATPase subunits in the D1 and D2 rings. Density for ADP/BeF$_x$ and neighboring protein segments are shown as a blue mesh. Models for protein are shown in ribbon representation and the nucleotides as stick models. Arg residues contacting the nucleotide from the neighboring ATPase subunits are indicated. The assignment of ADP or ADP-BeF$_X$ is based on comparing nucleotide densities and the presence or absence of an Arg finger of the neighboring subunit in its vicinity. Density for subunits F of both rings is weak and therefore not shown. These subunits are probably in the nucleotide-free state.

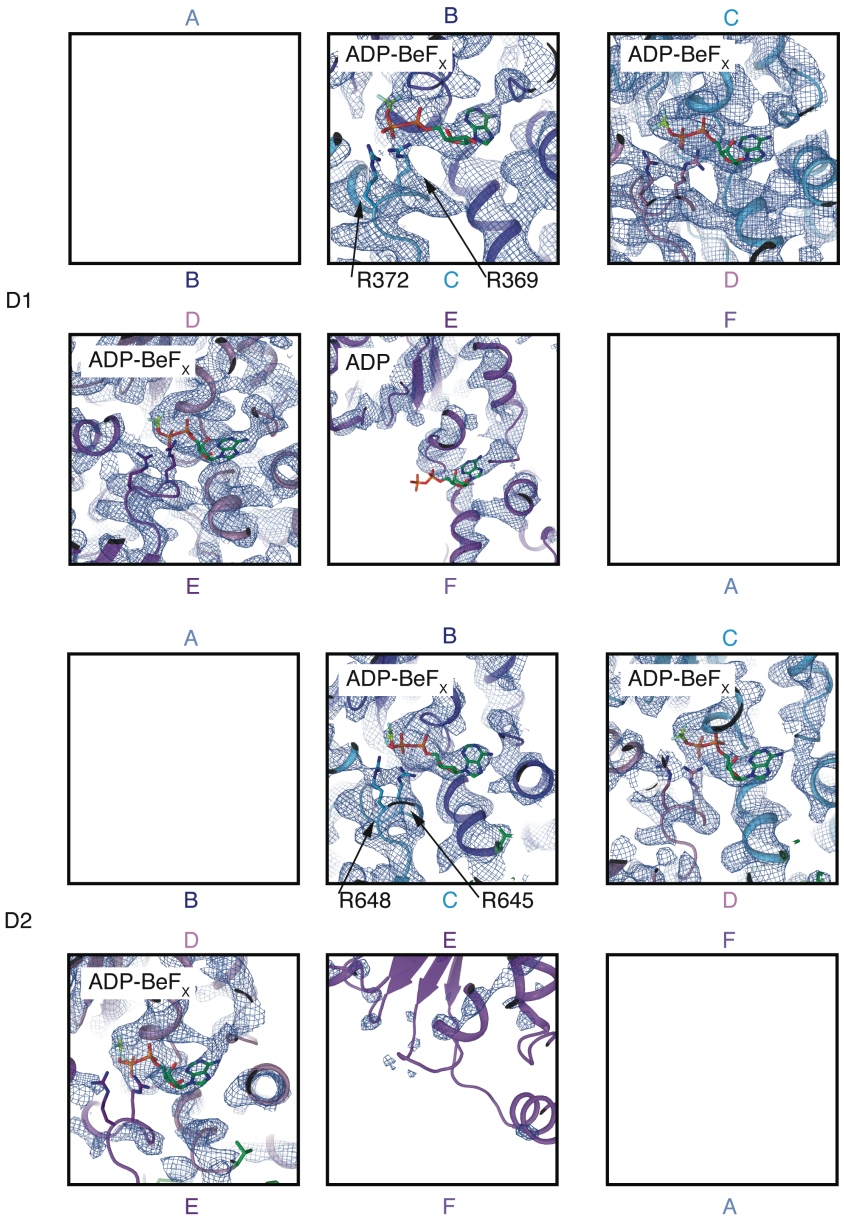

Fig. S17. Nucleotides bound in the ADP/BeF$_x$-1 structure.

Nucleotide binding pockets of the ATPase subunits in the D1 and D2 rings. Density for ADP/BeFx and neighboring protein segments are shown as a blue mesh. Models for protein are shown in ribbon representation and the nucleotides as stick models. Arg residues contacting the nucleotide from the neighboring ATPase subunits are indicated. The assignment of ADP or ADP-BeF$_X$ is based on comparing nucleotide densities and the presence or absence of an Arg finger of the neighboring subunit in its vicinity. Density for subunits A and F of both rings is weak and therefore not shown. These subunits are probably in the nucleotide-free state.

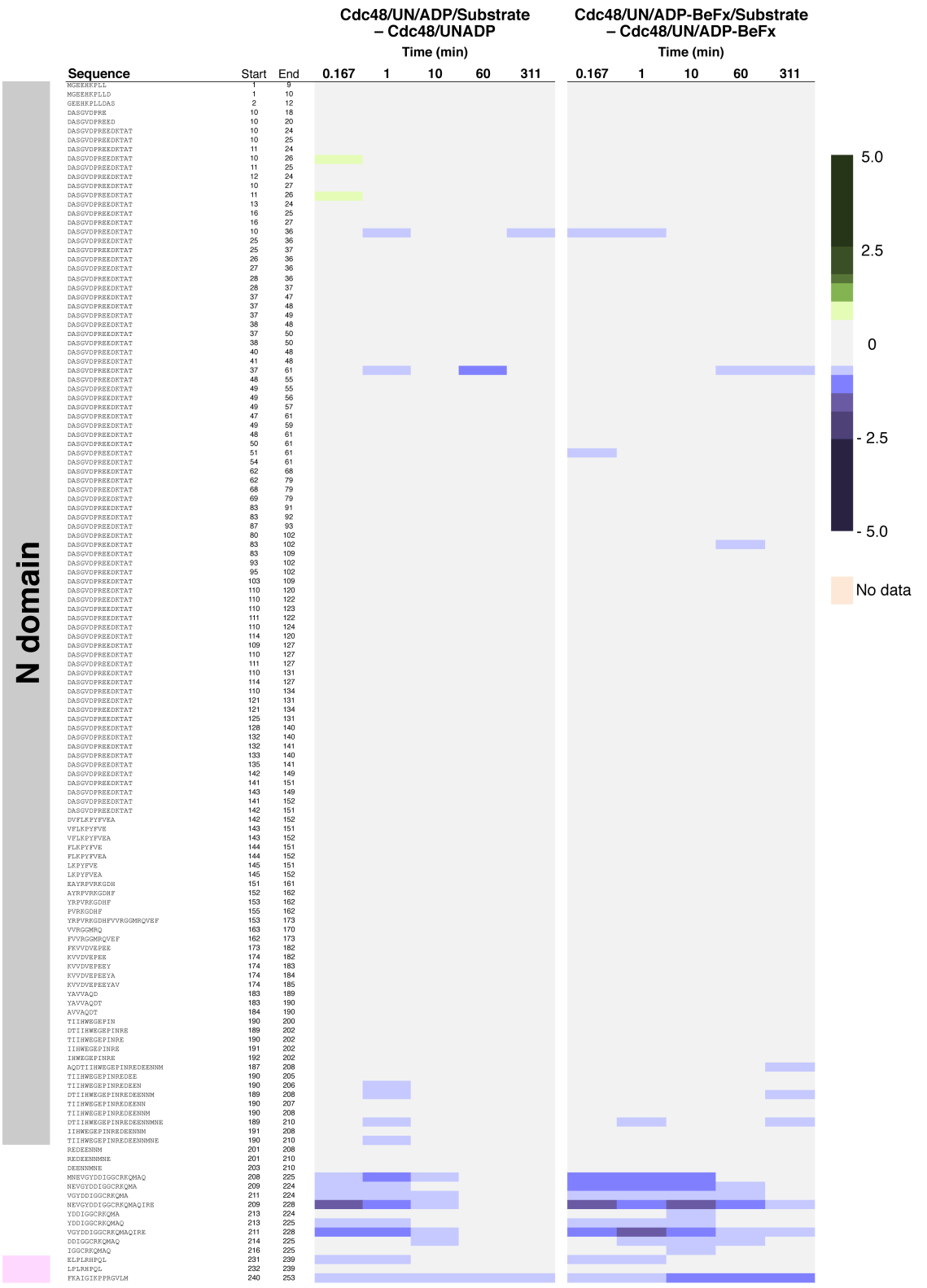

(Continued on next page)

(Continued on next page)

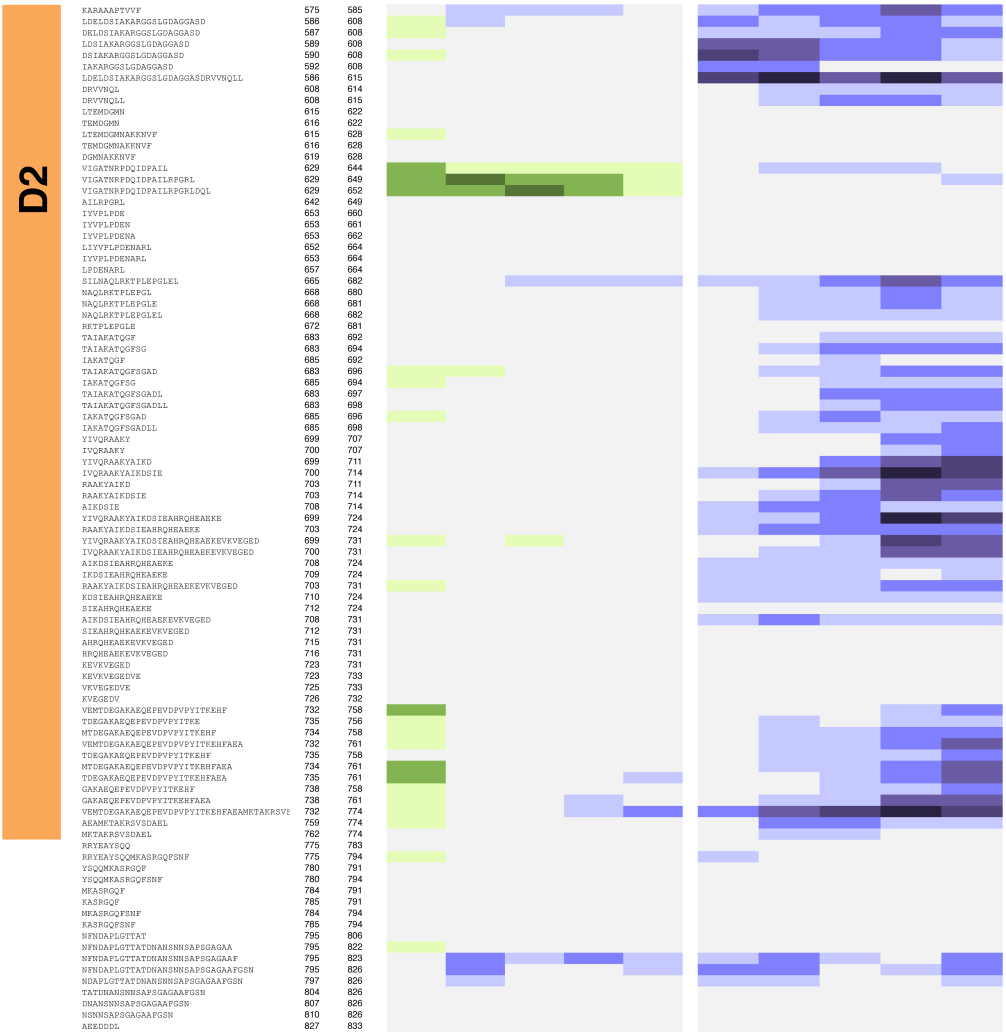

Fig. S18. Substrate protection of Cdc48 from HDX.

HDX was performed with a substrate-engaged Cdc48/UN complex and with substrate-lacking Cdc48/UN complex in the presence of ADP or ADP/BeF_x. The HDX reaction was quenched at different time points, the protein was digested with pepsin and the peptides analyzed by MS. Shown is the difference in HDX (with/without substrate) for peptides of Cdc48. Shown is the mean of two experiments. The peptides are listed from the N- to the C-terminus. The degree of HDX protection by substrate is shown in shades of blue (protection) and green (de-protection) (in Daltons, scale on the right). Peptides belonging to the N-, D1, or D2 domains are indicated by the bars on the left.

Table S1. Statistics for data collection and refinement

Structure	ATP	ADP/BeF_x-1	ADP/BeF_x-2
Data Accession			
PDB	6OA9	6OAA	6OAB
EMDB	EMD-0665	EMD-0666	EMD-20000
Data Collection			
Microscope	Titan Krios	Talos Arctica	
Voltage (kV)	300	200	
Exposure navigation	Stage Movement	Stage Movement	
Automation software	SerialEM	SerialEM	
Detector	Gatan K2 Summit (Super resolution)	Gatan K2 Summit (Counting)	
Energy filter	20 eV	N/A	
Pixel Size	0.675 Å	1.15 Å	
Exposure time, frames	10.0 s, 50 frames	8.0 s, 40 frames	
Dose rate ($e^- pixel^{-1} s^{-1}$)	10.0	7.4	
Electron exposure ($e^-/Å^2$)	54.9	44.7	
Defocus range (μm)	-1.0 to -2.5	-1.0 to -2.5	
Micrographs collected	3037	2523	
Reconstruction			
Software	Cryosparc2	Cryosparc2	
Micrographs used	2772	1772	
Particles extracted	1,588,559	1,017,931	
Particles used	127,261	30,118	93,395
Box Size (pixels)	200	234	
Symmetry	C1	C1	
Overall resolution (Å)		4.1	3.6
FSC=0.5 (masked/unmasked, Å)	4.3/7.3	4.9/11.6	3.9/6.8
FSC=0.143 (masked/unmasked, Å)	3.9/3.6	4.1/6.6	3.6/4.5
Map sharpening B-factor ($Å^2$)	-150	-150	-100
Local resolution range (Å)	3.0 to 9.7	3.0 to 10.0	2.5 to 9.0
Model Refinement			
Software	Phenix	Phenix	
R.M.S. deviations			
Bond length (Å)	0.01	0.01	0.01
Bond angle (°)	0.97	1.1	0.85
Ramachandran statistics (%)			
Outliers	0.08	0.16	0.08
Allowed	6.38	8.07	7.77
Favored	93.54	91.77	92.15
MolProbity score	1.71	1.84	1.75
All-atom clashscore	5.31	6.33	5.13
Poor rotamers (%)	0.16	0.14	0.24
B-factors (Protein/Ligand)	258.49/127.51	112.30/98.51	93.22/81.82
Map correlation coefficient	0.784	0.790	0.754
Model vs. Map FSC			
FSC=0.5 (masked/unmasked, Å)	4.20/4.21	4.29/4.32	3.91/3.96
FSC=0.143 (masked/unmasked, Å)	3.86/3.88	4.06/4.10	3.63/3.65